OFFICE OF NAVAL RESEARCH

Contract N00014-82-K-0280

Task No. NR413E001

TECHNICAL REPORT NO. 30

An ESDIAD Study of Chemisorbed Hydrogen on Clean and H-Exposed Si(111)-(7x7)

by

R.M.Wallace, P.A.Taylor, W.J.Choyke and J.T.Yates, Jr.

Submitted to

Surface Science

Surface Science Center
Department of Chemistry
University of Pittsburgh
Pittsburgh, PA 15260

11 May 1990

UNCLASSIFIED
SECURITY CLASSIFICATION OF THIS PAGE (When Data Entered)

MASTER COPY - FOR REPRODUCTION PURPOSES

REPORT DOCUMENTATION PAGE		READ INSTRUCTIONS BEFORE COMPLETING FORM
1. REPORT NUMBER: 30	2. GOVT ACCESSION NO.	3. RECIPIENT'S CATALOG NUMBER
4. TITLE (and Subtitle): An ESDIAD Study of Chemisorbed Hydrogen on Clean and H-Exposed Si(111)-(7x7)		5. TYPE OF REPORT & PERIOD COVERED
		6. PERFORMING ORG. REPORT NUMBER
7. AUTHOR(s): R.M.Wallace, P.A.Taylor, W.J.Choyke and J.T.Yates, Jr.		8. CONTRACT OR GRANT NUMBER(s)
9. PERFORMING ORGANIZATION NAME AND ADDRESS: Surface Science Center, Chemistry Department, University of Pittsburgh, Pittsburgh, PA 15213		10. PROGRAM ELEMENT, PROJECT, TASK AREA & WORK UNIT NUMBERS
11. CONTROLLING OFFICE NAME AND ADDRESS		12. REPORT DATE: 5/11/90
		13. NUMBER OF PAGES: 34
14. MONITORING AGENCY NAME & ADDRESS (if different from Controlling Office)		15. SECURITY CLASS. (of this report): Unclassified
		15a. DECLASSIFICATION/DOWNGRADING SCHEDULE

16. DISTRIBUTION STATEMENT (of this Report)

17. DISTRIBUTION STATEMENT (of the abstract entered in Block 20, if different from Report)

18. SUPPLEMENTARY NOTES

- Distribution (ESDIAD) (JG)

19. KEY WORDS (Continue on reverse side if necessary and identify by block number)

Silicon
Hydrogen
Silane
Atomic H
Dangling Bonds

Physical Chemistry, Surface Properties, Crystal Structures, Semiconducting Films, Electron-Stimulated Desorption Ion Angular

20. ABSTRACT (Continue on rev)

The chemisorption of H on Si(111)-(7x7) has been studied by digital ESDIAD and temperature programmed desorption methods. It has been found that residual H in the bulk of the Si(111) can be transported to the surface upon annealing to temperatures above ~1000 K. The adsorption of atomic H on Si(111)-(7x7) results in a mixture of monohydride and polyhydride species as detected by H+ ESDIAD. Thermal desorption from the H-saturated surface liberates β_3-H_2, β_2- and β_1-H_2 species as well as SiH_4(g). Heating the H-saturated surface to 1040 K results in a significant disordering of the surface, leading to Si sites which produce highly tilted Si-H bond directions. The occupation of these sites with H produces surface species exhibiting high polar angles from the surface normal for H+ desorption by an ESD process with a high ionic cross section compared to the cross section observed for normal mono- and polyhydride surface species.

H(+)

DD FORM 1 JAN 73 1473 EDITION OF 1 NOV 65 IS OBSOLETE

UNCLASSIFIED
SECURITY CLASSIFICATION OF THIS PAGE (When Data Entered)

(Bd a. 3(-), Ed a. 2(-), B1-112)

Submitted to: Surface Science

Date: 11 May 1990

An ESDIAD Study of Chemisorbed Hydrogen on Clean and H-Exposed Si(111)-(7x7)

R.M.Wallace, P.A.Taylor, W.J.Choyke and J.T.Yates, Jr.

Surface Science Center
Department of Chemistry
University of Pittsburgh
Pittsburgh, PA 15260

An ESDIAD Study of Chemisorbed Hydrogen on Clean and H-Exposed Si(111)-(7x7)

R.M.Wallace, P.A.Taylor, W.J.Choyke and J.T.Yates, Jr.

Surface Science Center
Department of Chemistry
University of Pittsburgh
Pittsburgh, PA 15260

Abstract

The chemisorption of H on Si(111)-(7x7) has been studied by digital ESDIAD and temperature programmed desorption methods. It has been found that residual H in the bulk of the Si(111) can be transported to the surface upon annealing to temperatures above ~1000 K. The adsorption of atomic H on Si(111)-(7x7) results in a mixture of monohydride and polyhydride species as detected by H^+ ESDIAD. Thermal desorption from the H-saturated surface liberates β_3-, β_2- and β_1-H_2 species as well as SiH_4(g). Heating the H-saturated surface to 1040 K results in a significant disordering of the surface, leading to Si sites which produce highly tilted Si-H bond directions. The occupation of these sites with H produces surface species exhibiting high polar angles from the surface normal for H^+ desorption by an ESD process with a high ionic cross section compared to the cross section observed for normal mono- and polyhydride surface species.

I. Introduction

The interaction of hydrogen with silicon surfaces, under investigation for over forty years [1], continues to be of interest because of the effect that hydrogen has on the electronic [2-6] and the structural properties [7] of crystalline (and poly-crystalline/amorphous) silicon. The interaction of hydrogen and silicon is also of interest in the mechanistic studies of semiconductor film growth processes, such as in chemical vapor deposition (CVD), where hydrogen is a ubiquitous component [8].

There have been numerous surface science investigations of the silicon-hydrogen system. These include absolute coverage measurements [9-11], high resolution electron energy loss spectroscopy (HREELS) [12-19], infrared absorption studies [20-28], molecular beam investigations [29,30], thermal desorption studies (TPD or TDS) [31-40], adsorption studies [1,41,42], photoemission studies [33,43-50], electron diffraction investigations [51,52], electron-stimulated desorption (ESD) studies [53-58], Auger electron spectroscopy (AES) studies [53,54,59,60], atom probe field ion microscopy investigations [61] and, recently, studies by scanning-tunneling microscopy (STM) [62-64].

From these studies, hydrogen is known to form SiH (monohydride), SiH_2 (dihydride) and SiH_3 (trihydride) surface species on Si(111) and Si(100). The formation of the surface dihydride and trihydride phases leads to a reconstruction of the silicon surface which necessarily involves the breaking of Si-Si bonds. Recent STM investigations of the H-saturated Si(111) surface, where SiH_2 and SiH_3 surface species exist, have indicated that significant surface disorder results from this Si-Si bond breaking and suggest that the relief of strain in the Si adatom backbond is accompanied by the formation of

the higher hydride phases [64]. Such disorder is not observed by STM when only the monohydride phase is present [62,63].

The complication of the surface disorder, induced by the formation of the higher hydride phases, has made the interpretation of the structural properties of the SiH_x surface layer by atomic resolution STM techniques difficult. Here we report the first electron-stimulated desorption ion angular distribution (ESDIAD) study of H^+ ion production from the clean and H-exposed Si(111)-(7x7) surface. This investigation has been carried out in order to examine the distribution of bonding geometries of the complex SiH_x surface layer. The ESDIAD technique permits the determination of adsorbate bonding directions for surfaces with a chemisorbed species of a single structural type by measuring the angle-resolved distributions of ESD-produced ion fragments from the adsorbate [65,66]. ESDIAD has only recently been applied to adsorbate-semiconductor systems [67-70].

We find that an Ar^+ ion bombarded and subsequently annealed Si(111) surface has a small concentration of residual surface hydrogen that originates from hydrogen diffusion from the bulk. This residual hydrogen produces a H^+ ESDIAD pattern that indicates the presence of non-normally oriented surface Si-H bonds. We also find that, upon exposure of the Si(111) surface to atomic hydrogen, the presence of the di- and trihydride phases on Si(111) results in the production of Si-H bond directions exhibiting large polar angles away from <111>. Removal of these polyhydrides, by thermal desorption, results in a higher population of more normally-oriented Si-H surface bonds, where a characteristic normally peaked H^+ ESDIAD pattern is observed. Further annealing to remove the monohydride phase results in a very broad H^+ ESDIAD pattern and indicates the presence of a mixture of very highly tilted Si-H bond directions. This observation suggests that the annealed surface has been substantially

disordered. This may be due to the scission of Si-Si bonds during the formation of the higher hydrides which subsequently decompose during annealing.

II. Experimental

The ultrahigh vacuum (UHV) chamber used in this study is described elsewhere [71]. The base pressure of the system is 4×10^{-11} Torr and the pumping time constant is estimated to be ~0.5 s. The chamber, shown in Fig. 1, is equipped with a scanning Auger electron spectrometer (AES), a line-of-sight, shielded quadrupole mass spectrometer (QMS) for thermal desorption studies, a digital LEED/ESDIAD apparatus, a second QMS for ESD studies, and a W-spiral filament for the production of atomic H from H_2.

The Si(111) crystal was Czochralski grown, 10 Ω-cm, p-type (B-doped) and cut from an oriented (~1°) wafer that was commercially polished. The crystal dimensions were 1.30x1.31x0.15 cm and the crystal was slotted on the edges for mounting as described elsewhere [71]. The crystal support structure was cooled by thermal contact with a small reservoir through which cooled N_2 gas flowed. The crystal was resistively heated with a programmable temperature controller. Crystal temperature was carefully monitored with a chromel-constantan (type-E) thermocouple enclosed in a small Ta-foil envelope that was inserted into one of the crystal slots [71]. Crystal temperatures between 120 K and 1200 K are readily produced, and temperature control to ±5 K is routinely achieved.

The crystal was cleaned after cutting of the crystal slots with the well-known chemical oxidation-HF stripping treatment [72,73], followed by a methanol rinse prior to installation in the UHV chamber. Final cleaning in UHV was accomplished by 2 kV Ar^+ ion bombardment at glancing incidence(10^{-3} Ccm^{-2}, C ≡ Coulomb) followed by annealing to 1173 K and cooling to 120 K. A sharp (7x7) LEED pattern was observed after this preparation procedure, and impurities

(e.g. C,N,O and Ni) were below detectable limits of the AES (<0.01 atomic fraction within the depth of Auger sampling).

For the hydrogen dosing experiments, a hot (T=1800 K) W-spiral filament (diameter=1 cm) was used to atomize molecular hydrogen. Hydrogen was admitted into the chamber to $P(H_2)\sim10^{-8}$ Torr, (uncorrected for ionization gauge sensitivity) and the crystal was placed ~4 cm from the spiral. Crystal temperatures remained below 340 K during these exposures, and the formation of the surface mono-, di-, and trihydride species was easily accomplished with this configuration. Exposures to atomic hydrogen are proportional to the H_2 exposures, and H_2 exposures are reported throughout this paper as Langmuirs (L) H_2 ($1L=1x10^{-6}$ Torr sec). From temperature programmed desorption (TPD) measurements of the H-exposed surface, a calibration of the surface coverage can be made in terms of the observed H_2 desorption features. Under the conditions described here, we have found that exposures greater than 3L are required to observe the onset of the dihydride (β_2) desorption feature. Thus, exposures larger than 3L result in the population of di- and trihydride phases and the observation (by TPD) of the β_2-H_2 and β_3-H_2 and SiH_4 (by the fragmentation products SiH^+, SiH_2^+ and SiH_3^+) desorption features. The crystal is biased at -100V during such exposures to eliminate the possibility of ESD effects from any stray electrons striking the surface.

Temperature programmed desorption (TPD) measurements were made with the shielded, differentially-pumped QMS described elsewhere [71]. The shielded QMS is equipped with two apertures: one large aperture (area~18.2 cm^2) used for random flux adsorption measurements and a small axially-located aperture (area~0.2 cm^2) used for line-of-sight TPD measurements. A rack-and-pinion driven sliding door for the large aperture was kept closed during TPD measurements. The small aperture to the shielded QMS was placed on the

line-of-sight axis between the Si(111) surface and the QMS ionizer at a distance of 0.2 cm from the crystal, and ensures that only species desorbing from the central area of the prepared Si(111) surface are detected. This aperture is electrically isolated so that it may be biased negatively to prevent the escape of stray electrons from the QMS ionizer which could lead to spurious ESD effects on the surface under examination.

Digital ESDIAD and LEED measurements of the clean and H-exposed surface were made with the apparatus shown in Fig. 2. The apparatus is equipped with a Comstock EG-401 electron gun and x-y deflection plates. Typically, a ~1 mm diameter electron beam impinges on the crystal with electron energies of 300 eV-400 eV and a current of $\sim 1 \times 10^{-8}$ A. The positive ions produced from this electron beam, by the ESD process, are intercepted by three hemispherical grids in the retarding field analyzer. For ESDIAD measurements, the grids are biased as follows: $V_1=V_2=0$ V, $V_3= 0.7(V_{xtal})$. The crystal potential for all of the ion desorption results reported here is $V_{xtal}=+100$ V. The ions then pass through two planar grids, $V_4=0$ V and $V_5=-500$ V, and are collected on a multichannel plate (MCP)/anode assembly which provides signal amplification. A gain of $\sim 10^5$ over the input ion current is achieved with the MCP/anode assembly. A current pulse, resulting from a shower of electrons that are in spatial registry in the MCP assembly with the incident ion, is collected on the resistive anode. The statistical distribution of the angles of ion desorption from the surface is digitally recorded for 10^6-10^7 desorbed ions [74,75]. The identity of the ESD-produced ions is determined with the second QMS which is equipped with an electron gun identical to that employed on the LEED/ESDIAD apparatus. This measurement is described fully elsewhere [71]. Only H^+ ions were detected (above noise levels) throughout this study. LEED measurements are made by simply changing the grid potentials to permit the detection of

elastically scattered electrons.

A background signal, due to the production of characteristic soft x-rays, or electronically excited neutral (metastable) species from the electron bombardment of the crystal, is also recorded for later background subtraction. The grid G_3 is biased at $+1.5(V_{xtal})$ for this measurement, thus permitting only the characteristic soft x-ray signal or other background signal to be collected. The background signal, which is unrelated to the H^+ ESDIAD signal, can be ~50% of the raw H^+ ESDIAD signal from Si, and must therefore be considered in a quantitative measurement. This background contribution to the ESDIAD data has been described elsewhere [76]. All of the H^+ ESDIAD results reported herein have had the background component subtracted, and all of the H^+ ESDIAD patterns shown have the same vertical scale.

III. Results

A. Measurements on the clean Si(111)-(7x7) surface

The ESDIAD of the clean Si(111)-(7x7) surface, prepared by the ion bombardment and annealing procedure described above, results in a broad H^+ ion angular distribution. This is shown in Fig. 3 for various crystal biasing potentials.

It is well known that the observed trajectories of the desorbing species can be perturbed by image force and reneutralization effects induced by the interaction of the desorbing species with metal substrates [77-80]. Such effects are expected to manifest themselves to some degree with semiconductor substrates as well [67,68]. By increasing the positive potential of the crystal, the trajectories of the desorbing positive ions are deflected toward the normal, and this effect is observed in the detected angular distribution, resulting in a "compression" of the observed ion angular distribution pattern.

The effect of pattern compression is shown in Fig. 3 where it is seen that as the crystal bias is increased to higher positive potentials, a central H^+ peak develops as H^+ ions with trajectories that are at large angles from the normal are compressed toward the normal. It is noted that even at V_{xtal}=+100V, the observed H^+ ESDIAD central pattern is rather broad with evidence of even larger-angle (with respect to the surface normal) H^+ desorption as indicated by the nonzero signal extending to the pattern perimeter. (The square-shaped edge of nonzero intensity is due to the detector geometry.) Thus the +100 V compression procedure is able to separate H^+ ions produced by ESD into two general groups - a broad distribution which may be detected close to the normal by employing the crystal bias, and an even broader H^+ distribution which persists at the +100 V bias. The H^+ intensity in the perimeter region is sensitive to crystal preparation and will be discussed below.

Temperature programmed desorption measurements of the clean, prepared Si(111)-(7x7) surface are shown in the inset of Fig. 4, where a small H_2 desorption feature is observed at T_{max}~830 K. The maximum desorption rate is observed at a temperature which is similar to that from the low coverage β_1-monohydride desorption on a H-exposed Si(111) surface. This suggests that the desorbing H_2 species is related to monohydride SiH surface species. In this experiment, the crystal is resistively heated with a linear temperature program (rate~1.6 K/s) to 1100 K and the thermal desorption of H_2 is monitored from the crystal center with the shielded, differentially-pumped QMS [71]. After the desorption measurement, the crystal is rotated away to prevent radiative heating of any nearby surfaces to avoid possible contamination from species (e.g. H_2O) desorbing from such surfaces and the crystal is cooled according to a linear program (~1 K/s) to 120 K. This "heat-rotate-cool" cycle was repeated five times (points (a)-(e) of Fig. 4) in order to examine the effect of heating

the crystal on the observed residual hydrogen desorption yield.

The residual hydrogen desorption yield from this experiment (dark points of Fig. 4) is observed to decrease with each subsequent TPD cycle indicating that the hydrogen (surface) species are slowly being depleted in the cycling process. For an approximate coverage comparison, the H_2 desorption yield from a saturated monohydride layer is shown as the open circle in Fig. 4. This suggests that ~0.1 monolayers (ML) of the clean, prepared Si(111)-(7x7) surface is initially populated with a SiH species, even after all cleaning procedures in UHV have been carried out. This also suggests that continual repopulation of surface SiH occurs in the sequential desorption experiments. In five sequential heating experiments, about 0.2 ML of H are evolved as H_2.

The possible source(s) of this residual H have been investigated with care. Although no evidence of hydrogenic impurities in the Ar gas used for ion bombardment has been found, residual H_2 and CH_4 in the vacuum system could lead to a fluence of hydrogen (as H_2^+, H^+, CH_4^+, CH_3^+, etc.) at a fluence of $\sim 5 \times 10^{-4}$ of the Ar^+ fluence used for cleaning the Si(111) crystal. Under these conditions, for a total Ar^+ fluence of 2×10^{-3} C cm^{-2}, approximately 6×10^{12} H cm^{-2} would be implanted, corresponding to ~0.02 ML of H. Additional sources of bulk hydrogen may originate from the wet chemical cleaning procedure employed, or from hydrogen trapped on B dopant sites, as will be discussed later. It should be noted that careful attention was given to hot filaments, etc. as a source of atomic hydrogen and of other active radical species in the UHV background. During the TPD measurements, only the shielded QMS ionizer filament is on, and the emission of stray electrons from the ionization source is retarded by applying -100 V to the shielded QMS entrance aperture. It should also be noted that, unlike atomic hydrogen, $H_2(g)$ has a very low sticking coefficient on Si [30], and background $H_2(g)$ cannot be a source of the residual

surface hydrogen observed.

Based on these measurements, and the results of others (discussed below), we believe that one plausible source of the surface hydrogen on the Si(111) crystal (cleaned as described above) is the diffusion of hydrogen to the surface from the bulk.

B. Measurements on the H-exposed Si(111) surface

The ESDIAD measurements for H^+ as a function H-exposure of the Si(111)-(7x7) surface is shown in Fig. 5. Exposures are reported in units of Langmuirs (L) of H_2. In Fig. 5 the compression voltage is +100 V. Fig 5(a) shows the ESDIAD pattern from the clean, prepared surface and indicates that a SiH species is initially present on this surface. It is noted that the H^+ peak intensity and the base intensity in the pattern perimeter of Fig. 5(a) is less evident compared to Fig. 3(f). We believe that this difference is due to differences in crystal preparation history and this will be discussed below. Increasing the exposure to 2.0 L (Fig. 5(c)), which corresponds to a nearly saturated monohydride phase, results in a broad, centrally-peaked compressed ESDIAD pattern. Further increasing the exposure into the di- and trihydride phases (Fig. 5 (d-f)) results in the appearance of large-angle H^+ desorption, as seen from the additional H^+ signal near the pattern perimeter. The average intensity of the signal in the pattern perimeter is ~10-20% of the central peak intensity for the hydrogen exposures that produce the di- and trihydride phases.

Temperature programmed desorption (TPD) studies of a 20.6 L exposure (corresponding to substantial formation of the SiH_2 and SiH_3 phases), which is similar to the coverage of Fig. 5 (f), are shown in Fig. 6. The well known desorption features due to the (β_2) dihydride (T_{max}~650 K) and the (β_1) monhydride (T_{max}~775 K) species are evident [33] as well as a β_3-desorption

process near 400 K. In agreement with Greenlief, et al., mass spectrometer fragmentation products from desorbing SiH_4 are observed near 600 K, indicating that the scission of Si-Si bonds (etching) has occurred [40]. Consistent with the work of ref. 40, we also note that the SiH_4 desorption (observed as SiH_3^+, SiH_2^+ and SiH^+) is initially observed at H atom exposures corresponding to the first appearence of the (β_2) dihydride phase [40].

The effect on the compressed H^+ ESDIAD pattern of heating the H-exposed surface is shown in Figs. 7 and 8. In all cases, after heating the surface to the indicated temperature, the crystal is cooled to 120 K before making ESDIAD measurements. In Fig. 7 (b-d), both the centrally oriented H^+ ESDIAD peak and the very broad H^+ pattern filling the perimeter regions (Fig. 7(e)) are observed. As a more quantitative measure of the ESDIAD central peak shape in Fig. 7(b-e), the peak width was determined using two methods: (1) the azimuthally-averaged width at the half maximum of the peak was measured, and (2) an average peak half width about the "center of mass" of the pattern was also measured. The results of these measurements are shown in Fig. 8. It is seen that both width measurement methods yield essentially the same peak width, indicating that the pattern has a circularly-symmetric cross section. The error bars shown represent the standard deviation from the average peak width measured.

The pattern shown in Fig. 7(a) is again that due to a clean, prepared crystal (see Fig. 5(a) and the subsequent discussion). Exposing the surface to atomic hydrogen (10 L H_2) results in the pattern shown in Fig. 7(b). This exposure results in the production of higher hydride phases on the surface and the pattern perimeter intensity increases to 10-20% of the central peak intensity. In the experiment shown in Fig. 7, the total H^+ ESDIAD yield from the exposed surface (Fig. 7(b)) is over an order of magnitude larger than that

from the "clean" surface (Fig. 7(a)). Other similar experiments (data not shown) have indicated that the clean surface H^+ ion yield behavior can vary considerably from experiment to experiment. Because extreme care was taken in reproducing atomic H exposures, we believe that this behavior is mainly due the crystal preparation history, although gain changes in the MCP/anode assembly have also been noted after lengthy hydrogen exposures.

As shown in Fig. 7(c), annealing the crystal to 601 K (just before the (β_2) dihydride H_2 desorption process shown in Fig. 6) with the linear temperature ramp has only a small effect on the compressed H^+ ESDIAD pattern. A small increase in integrated peak intensity and the very broad angular H^+ distribution in the perimeter region is again observed. The peak width remains essentially constant after this annealing procedure, as shown in Fig. 8.

However, increasing the temperature to 710 K (the temperature corresponding to the minimum between the (β_2) dihydride and the (β_1) monohydride thermal desorption features of Fig. 6) results in a sharpening of the central H^+ peak (Fig. 7(d)) as shown by the ~20% decrease in the measured peak width in Fig. 8. The central peak sharpens although the intensity in the pattern perimeter region, which is due to large angle H^+ desorption, remains significant (~20% of the central peak intensity).

Annealing the crystal to 1041 K, beyond the monohydride desorption feature, results in a very broad and intense H^+ angular distribution (Fig. 7(e)), unlike any of those previously observed. Such an H^+ ESDIAD pattern is consistent with a distribution of Si-H bond directions at very large angles from the normal. The ESD process responsible for this pattern occurs with an enhanced ionic cross section. The observation of this very broad and intense H^+ ESDIAD pattern after the removal of the β_1 phase by thermal desorption was reproducible in all of the experiments performed.

The broad H^+ ESDIAD pattern can be eliminated by annealing the Si(111) surface in vacuum at 1173 K. For the experiment shown in Fig. 7, the initial H^+ pattern (Fig. 7(a)) closely resembles that produced by annealing alone, but, in this particular case, Ar^+ bombardment followed by annealing to 1173 K was employed.

IV. Discussion

A. Source of surface H on "clean" Si(111)

Several plausible sources of the observed surface hydrogen can be suggested and include: (1) surface preparation, including hydrogenic impurity implantation during Ar^+ sputtering; (2) the presence of hydrogen during crystal growth; and (3) re-exposure of the surface to atomic hydrogen in UHV. Recently, much attention has been given to the microscopic morphology of Si surfaces, particularly those prepared with the well known chemical oxidation/HF stripping technique [72,73]. After such preparation, others have found a remarkably passive, H-terminated layer [81] and various silicon hydride species are observed on the surface [26,82]. Surfaces generated by this wet chemical cleaning technique have also been shown to be stepped and to undergo oxidation in the air only after several hours [83].

From our initial cleaning procedure prior to installation in the UHV system, such a hydrogen-terminated surface is expected and may serve as a possible initial source for the residual $H_2(g)$ desorption feature observed in our TPD results (Fig. 4) and the ESDIAD results yielding H^+ (Fig. 3, for example) reported here even after annealing at 1173 K. This surface hydrogen, as well as bulk hydrogen which may be initially present in the crystal, will be redistributed as a result of Ar^+ bombardment of the Si(111) crystal, and this

hydrogen along with H introduced by background gases present during Ar^+ bombardment could be a source of the residual surface hydrogen observed by TPD and ESDIAD in these experiments. Indeed, others have shown that the solubility of hydrogen in Si increases due to the presence of a high dislocation density [84].

The propensity for bulk hydrogen in Si to form boron-hydride complexes has also been examined by others [2-5], and may be of importance as a source of our residual hydrogen. The thermal desorption data of Fig. 4 suggests that a small surface concentration of H (~0.1 ML) is initially present after the ion-bombardment/annealing procedure described previously. This would correspond to ~$3x10^{13}$ H/cm^2 (where $3x10^{14}$ d-b/cm^2 is the dangling bond (d-b) density on the ideal Si(111) surface) assuming that 1 ML of H corresponds to a saturation of these dangling bonds. Our p-type, B-doped samples have a nominal resistivity of 10 Ω-cm which would correspond to roughly 10^{15} B/cm^3 [85] and thus provide a bulk reservoir for B-H complexes that could provide one source for H diffusion to the surface.

High temperature transport of hydrogen in crystalline Si is known to occur. For example, assuming a diffusion coefficient of $D=10^{-4}$ cm^2/s at T=1173 K [85] and typical annealing times of τ~300 s, a diffusion length of $(D\tau)^{1/2}$=0.17 cm is obtained. With our crystal thickness in the <111> direction of 0.15 cm, hydrogen diffusion throughout the crystal is expected to readily take place during such annealing. The observed depletion of the surface Si-H species with subsequent annealing cycles is also consistent with a bulk source of hydrogen that is diffusion rate limited.

Of course, further re-exposure of the Si surface to atomic hydrogen in our experiments may also provide a means for some amount of surface hydrogen to diffuse into the bulk and again reappear on the surface after the ion

bombardment/annealing procedure used to prepare the surface. It is noted, for example, that the ESDIAD data of Fig. 3(f) and that of Fig. 5(a) (or Fig. 7(a)), in which the H^+ yield is clearly different, suggests that crystal preparation history affects the concentration of residual surface hydrogen which may be achieved by delivery from the bulk.

B. ESDIAD of the "clean" Si(111) surface

Many of the common surface science measurement techniques are unable to easily detect the presence of surface hydrogen. Electron stimulated desorption, however, has been shown to be a sensitive probe for hydrogen on clean Si surfaces [55,57]. The ESDIAD results shown in Fig. 3 for the "clean" Si(111) surface clearly indicate the presence of a surface SiH species of two general types. The broad H^+ angular distribution at zero crystal bias indicates that non-normally oriented SiH species are observed. Compression of the pattern by positive electrical biasing of the crystal causes some of these widely-directed H^+ trajectories to coalesce about the normal to the crystal, as the H^+ ions are separated into two general groups - those which are compressed into a central H^+ peak and those which are not.

C. H-exposed Si(111)-(7x7)

Increasing the exposure (coverage) of hydrogen on the surface at 340 K, shown in Fig. 5, results first in the occupation of the monhydride phase, followed by the population of the dihydride and trihydride surface phases on Si(111)[40] (and Si(100),[38,39]). For coverages below the saturated monohydride phase (Fig. 5(b-c)), a broad, central peak is observed in the compressed ESDIAD pattern. This indicates that no preferential Si-H azimuthal directions are detected, and that a broad angular distribution of H^+ desorption

directions may be coalesced into the central peak by electrostatic pattern compression.

As the di- and trihydride species are formed at higher exposures (Fig. 5(d-f)), very large-angle H^+ desorption is also observed in the perimeter of the ESDIAD pattern. This perimeter region is largely unpopulated in the clean (Fig. 5(a)) and monohydride-exposed (Fig. 5(b-c)) H^+ ESDIAD patterns. This result suggests that Si-H bonding geometries, which lead to the observed off-normal H^+ angular distributions, are present and may be due to the surface dihydride and trihydride species as well as to possible tilted monohydride species. Such surface species have been observed recently for room temperature adsorption of atomic hydrogen on Si(111) [27]. The TPD measurements of the desorption of SiH_4 species (Fig. 6) also support this suggestion [40].

These results for the H-saturated Si(111) surface are also consistent with recent (room temperature adsorption) STM studies where adatom dihydride and adatom trihydride species are postulated [64]. Such species would be expected to give off-normal H^+ desorption in ESDIAD.

D. Si-H bonding direction- dependence on annealing

In Figs. 7 and 8, the geometry of the surface hydrides is examined with ESDIAD as a function of annealing the crystal followed by cooling to 120 K. Annealing the H-exposed surface (10 L) to 601 K (Fig. 7(c) and Fig. 8), the onset temperature for the dihydride (β_2-H_2) desorption process (see Fig. 6), results in little change in the observed ESDIAD pattern. The central peak intensity increases slightly with the peak width remaining constant. Very large-angle H^+ desorption is observed to produce H^+ intensity in the pattern perimeter. However, annealing to 710 K (Fig. 7(d) and Fig. 8), corresponding to the minimum between the dihydride and monohydride thermal desorption features

(see Fig. 6), results in a sharpening of the central ESDIAD peak, although very large-angle H^+ emission is also clearly observed. The central ESDIAD peak width decreases by ~20% and suggests that a distribution of Si-H bond angles corresponding to a higher relative population of more normally-oriented Si-H species is present. These results are also consistent with recent STM observations where a more structured surface is observed after removal of the polyhydride phases [64].

Further annealing to 1041 K, beyond the desorption of the (β_1) monohydride phase, results in a very broad H^+ ESDIAD pattern of high relative intensity, and is indicative of a mixture of randomly oriented Si-H species. Because Si-Si bond scission is expected to take place upon the formation of the higher hydride species which results in the evolution of SiH_4 thermal desorption products, substantial surface disorder is anticipated following thermal desorption for a hydrogen-covered surface. Such surface disorder (etching) would offer Si sites producing a variety of Si-H bonding directions.

Thus we have the rather surprising result that desorption of the polyhydride (β_3 and β_2) and the (β_1) monohydride phase does not completely depopulate surface H as measured by H^+ ESDIAD (and also by TPD, see Fig. 4). This residual surface hydrogen exhibits two distinct properties observable by ESDIAD:

1. Si-H bond angles which are directed very far from the Si(111) normal.
2. High relative H^+ ionic cross section in ESD as may be judged by comparison of the total yield of the ESDIAD pattern in Fig. 7(e) with other patterns at higher H coverages (Fig. 7(a-d)).

V. Summary

Both ESDIAD and TPD measurements have been employed to examine hydrogen

chemisorbed on Si(111)-(7x7). The following general observations were made:

1. Residual H originating from the bulk of the Si(111) crystal is responsible for the production of an H^+ ESD product even after annealing to 1173 K. The delivery of this residual H to the surface, with subsequent desorption of small fractions of a monolayer of H as H_2, is observed using TPD.
2. A mixture of monohydride and polyhydride surface species is detected by ESDIAD following the adsorption of atomic H. Polyhydride species are postulated to yield H^+ ESDIAD patterns having very broad angular distributions.
3. Thermal desorption from a hydrogen-saturated Si(111) surface is observed to liberate β_3-, β_2-, and β_1-H_2 above ~400 K. In addition, SiH_4(g) is liberated. Heating to 1041 K results in a significant disordering of the surface, producing Si adsorption sites which are capable of producing highly tilted Si-H bonds relative to the Si(111) normal. Adsorption of residual H on these Si sites results in species with large angles of H^+ desorption by ESD, and also with relatively high ionic cross sections for H^+ formation.

Acknowledgements

The authors acknowledge the full support of the Office of Naval Research for this work. The authors also thank Mr. C.-C. Cheng for useful discussions, and for the provision by Dr. John Bolland of a manuscript prior to publication.

References

a) Dept. of Physics, University of Pittsburgh, Pittsburgh PA.

1. J.T.Law, J. Chem. Phys. 30 (1959) 1568.
2. K.J.Chang and D.J.Chadi, Phys. Rev. B46 (1989) 11644.
3. J.I.Pankove, C.W.Magee and R.O.Wance, Appl. Phys. Lett. 47 (1985) 748.
4. J.I.Pankove, P.J.Zanzucchi, C.W.Magee and G.Lucovsky, Appl. Phys. Lett. 46 (1985) 421.
5. M.Stutzmann, Phys. Rev. B35 (1987) 5921.
6. C.H.Seager and R.A.Anderson, Appl. Phys. Lett. 53 (1988) 1181.
7. K.Christmann, Surf. Sci. Rep. 9 (1988) 1; and references therein.
8. J.M.Jasinski, B.S.Meyerson and B.A.Scott, Ann. Rev. Phys. Chem. 38 (1987) 109; and references therein.
9. R.J.Culbertson, L.C.Feldman and P.J.Silverman, J. Vac. Sci. Technol. 20 (1982) 868.
10. I.Stengaard, L.C.Feldman and P.J.Silverman, Surf. Sci. 102 (1981) 1; Nucl. Inst. Meth. 168 (1980) 589.
11. K.Oura, J.Yamane, K.Uzezawa, M.Naitoh, F.Shoji and T.Hanawa, Phys. Rev. B41 (1990) 1200.
12. H.Froitzheim, H.Ibach and S.Lehwald, Phys. Lett. 55A (1975) 247.
13. H.Wagner, R.Butz, U.Backes and D.Bruchman, Sol. St. Comm. 38 (1981) 1155.
14. H.Froitzheim, H.Lammering and H.L.Gunter, Phys. Rev. B27 (1983) 2278.
15. H.Kobayashi, K.Edamoto, M.Onchi and M.Nishijima, J. Chem. Phys. 78 (1983) 7429.
16. J.A.Schaefer, F.Stucki, J.A.Anderson, G.J.Lapeyre, and W.Göpel, Surf. Sci. 140 (1984) 207.

17. R.Butz, E.M.Oillig, H.Ibach and H.Wagner, Surf. Sci. 147 (1984) 343.

18. H.Froitzheim, U.Kohler and H.Lammering, Surf. Sci. 149 (1985) 537.

19. M.Nishijima, K.Edomoto, Y.Kubota, H.Kobayashi and M.Onchi, Surf. Sci. 158 (1985) 422.

20. Y.J.Chabal, Phys. Rev. Lett. 50 (1983) 1850.

21. Y.J.Chabal, E.E.Chaban and S.B.Christman, J. Electr. Spectr. Rel. Phenom. 29 (1983) 35.

22. Y.J.Chabal, G.S.Higashi and S.B.Christman, Phys. Rev. B28 (1983) 4472.

23. Y.J.Chabal and K.Raghavachari, Phys. Rev. Lett. 53 (1984) 282; Phys. Rev. Lett. 54 (1985) 1055.

24. J.C.Tully, Y.J.Chabal, K.Raghavachari, J.M.Bowman and R.R.Lucchese, Phys. Rev. B31 (1985) 1184.

25. Y.J.Chabal, Surf. Sci. 168 (1986) 594.

26. V.A.Burrows, Y.J.Chabal, G.S.Higashi, K.Raghavachari and S.B.Christman, Appl. Phys. Lett. 53 (1988) 998.

27. U.Jansson and K.J.Uram, to be published.

28. K.J.Uram and U.Jansson, to be published.

29. D.R.Olander, M.Balooch, J.Abrefah and W.J.Siekhaus, J. Vac. Sci. Technol. B5 (1987) 1404.

30. J.Abrefah and D.R.Olander, Surf. Sci. 209 (1989) 291.

31. Ch. Kleint, B.Hartmann and H.Meyer, Z. Phys. Chemie., Leipzig 250 (1972) 315.

32. K.D.Brzoska and Ch.Kleint, Thin Sol. Films 34 (1976) 131.

33. G.Schulze and M.Henzler, Surf. Sci. 124 (1983) 336.

34. X.Jin, Y.Feng, C.Zhuang and X.Wang, Acta Phys. Sin. 33 (1984) 746.

35. J. Leifels, Diplomarbeit, Univ. Hannover (1984).

36. B.G.Koehler, C.H.Mak, D.A.Arthur, P.A.Coon and S.M.George, J. Chem. Phys. 89 (1988) 1709.

37. K.Sinnah, M.G.Sherman, L.B.Lewis, W.H.Weinberg, J.T.Yates, Jr. and K.C.Janda, Phys. Rev. Lett. 62 (1989) 567; accepted J. Chem. Phys. (1990).

38. C.M.Greenlief, S.M.Gates and P.A.Holbert, J. Vac. Sci. Technol. A7 (1989) 1845.

39. S.M.Gates, R.R.Kuntz and C.M.Greenlief, Surf. Sci. 207 (1989) 364.

40. C.M.Greenlief, S.M.Gates and P.A.Holbert, Chem. Phys. Lett. 159 (1989) 202.

41. Yu. I. Belyakov, N.I.Ionov and T.N.Kompaniets, Sov. Phys. Sol. St. 14 (1973) 2567.

42. Ch. Kleint, Vacuum 36 (1986) 267.

43. H.Ibach and J.E.Rowe, Surf. Sci. 43 (1974) 481.

44. T.Sakurai and H.D.Hagstrum, Phys. Rev. B12 (1975) 5349.

45. K.C.Pandey, T.Sakurai and H.D.Hagstrum, Phys. Rev. Lett. 35 (1975) 1728.

46. J.A.Appelbaum, H.D.Hagstrum, D.R.Hamann and T.Sakurai, Surf. Sci. 58 (1976) 479.

47. T.Sakurai and H.D.Hagstrum, Phys. Rev. B14 (1976) 1593.

48. K.Fujiwara, Phys. Rev. B26 (1982) 2036.

49. D.Muller, F.Ringeisen, J.J.Koulmann and D.Bolmaont, Surf. Sci. 189/190 (1987) 472.

50. L.S.O.Johansson, R.I.G.Uhrberg and G.V.Hanaaon, Surf. Sci. 189/190 (1987) 479.

51. S.J.White and D.P.Woodruff, J. Phys. C9, (1976) 1451.

52. A.Ichimiya and S.Mizuno, Surf. Sci. 191 (1987) L765.

53. H.H.Madden, Surf. Sci. 105 (1981) 129.

54. H.H.Madden, D.R.Jennison, M.M.Traum, G.Margaritondo and N.G.Stoffel, Rev. B26 (1982) 896.

55. M.L.Knotek and J.E.Houston, J. Vac. Sci. Technol. B1 (1983) 899.

56. N.Matsunami, Y.Hasebe and N.Itoh, Surf. Sci. 192 (1987) 27.

57. C.F.Corallo and G.B.Hoflund, Surf. Int. Anal. 12 (1988) 297.

58. E.C.Ekwelundu and A.Ignatiev, Surf. Sci. 215 (1989) 91.

59. G.Allie, C.Lauroz and A.Cheneuas-Paule, Appl. Surf. Sci. 4 (1980) 221; J. Non Cryst. Sol. 35/36 (1980) 267.

60. A.Thanailakis, D.E.Ioannov and C.M.Reed, Sol. St. Comm. 44 (1982) 669.

61. T.Sakurai, E.W.Muller, R.J.Culbertson and A.J.Melmed, Phys. Rev. Lett. 39 (1977) 578.

62. T.Sakurai, Y.Hasegawa, T.Hashizume, I.Kamiya, T.Ide, I.Sumita, H.W.Pickering and S.Hyodo, J. Vac. Sci. Tecnol. A8 (1990) 259.

63. T.Tokumoto, K.Miki, H.Murakami, H.Bando, M.Ono and K.Kajimura, J. Vac. SCi. Technol. A8 (1990) 255.

64. J.J.Bolland, to be published.

65. T.E.Madey, Science 234 (1986) 316.

66. R.H.Stulen, Prog. Surf. Sci. 32 (1989) 1.

67. M.J.Dresser, P.A.Taylor, R.M.Wallace, W.J.Choyke and J.T.Yates, Jr., Surf. Sci. 218 (1989) 75.

68. A.L.Johnson, M.M.Walczak and T.E.Madey, Langmuir 4 (1988) 277.

69. M.J.Bozack, M.J.Dresser, W.J.Choyke, P.A.Taylor and J.T.Yates, Jr., Surf. Sci. 206 (1988) L833.

70. A.V.Hamza, G.D.Kubiak and R.H.Stulen, Surf. Sci. 206 (1988) L833.

71. R.M.Wallace, P.A.Taylor, W.J.Choyke and J.T.Yates, Jr., submitted J. Appl. Phys.; see also M.J.Bozack, L.Muehlhoff, J.N.Russell, W.J.Choyke and J.T.Yates, Jr., J. Vac. Sci. Technol. A5 (1987) 1.

72. W.Kern and D.A.Puotinen, RCA Rev. 31 (1970) 187.

73. W.Kern, RCA Engineer 28-4 (1983) 99; Semiconducor International, April 1984, 94.

74. M.J.Dresser, M.D.Alvey and J.T.Yates, Jr., Surf. Sci. 169 (1986) 91.

75. M.J.Dresser, M.D.Alvey and J.T.Yates, Jr., J. Vac. Sci. Technol. A4 (1986) 1446.

76. R.M.Wallace, M.J.Dresser, P.A.Taylor, W.J.Choyke and J.T.Yates, Jr., submitted, Rev. Sci. Instrum.

77. W.L.Clinton, Surf. Sci. 112 (1981) L791.

78. Z.Misković, J.Vukanić and T.E.Madey, Surf. Sci. 141 (1984) 285.

79. T.E.Madey, D.E.Ramaker and R.Stockbauer, Ann. Rev. Phys. Chem. 35 (1984) 215.

80. Z.Misković, J.Vukanić and T.E.Madey, Surf. Sci. 169 (1986) 405.

81. E.Yablonovitch, D.L.Allara, C.C.Chang, T.Gmitter and T.B.Bright, Phys. Rev. Lett. 57 (1986) 249.

82. Y.J.Chabal, G.S.Higashi, K.Raghavachari and V.A.Burrows, J. Vac. Sci. Technol. A7 (1989) 2104.

83. M.Niwa, H.Iwasaki and S.Hasegawa, J. Vac. Sci. Technol., A8 (1990) 266.

84. C.Kisielowski-Kemmerich and W.Beyer, J. Appl. Phys. 66 (1989) 552.

85. F.Shimura, Semiconductor Silicon Crystal Technology, Academic Press, San Diego,CA (1989) 266.

Figure Captions

Figure 1. Overview of UHV chamber used in this study. Base pressure of the system is 4×10^{-11} Torr.

Figure 2. Cross-sectional view of digital LEED/ESDIAD apparatus.

Figure 3. Effect of crystal bias on H^+ ion trajectories from "clean" Si(111)-(7x7). A gradual compression of the ESDIAD pattern is observed producing a central H^+ peak. In addition H^+ which does not coalesce into the central peak is observed in the perimeter of the pattern. All data taken at T=120 K with a 1×10^{-8} A, 400 eV electron beam. Elapsed time of data acquisition is 120 s. The crystal has been Ar^+ bombarded then annealed to 1173 K for 5 min.

Figure 4. Thermal desorption yield measurements for successive annealing cycles of "clean" Si(111)-(7x7) (see text). Inset: Temperature programmed desorption from the clean, prepared surface (dT/dt=1.6 K/s). The crystal has been Ar^+ bombarded then annealed to 1173 K for 5 min. prior to experiment (a).

Figure 5. ESDIAD from H-exposed Si(111). Exposures are reported in Langmuirs of H_2. All data taken at T=120 K with 1×10^{-8} A, 300 eV electron beam. Elapsed time of data acquisition is 120 s.

Figure 6. Temperature programmed desorption from H-saturated Si(111) (dT/dt=1.6 K/s). Only H_2(g) and the QMS fragments of SiH_4(g) (i.e. SiH_3^+, SiH_2^+ and SiH^+) are observed. Note the observation of desorbing species originating from SiH_4 product, indicating the removal of Si atoms (etching) from the surface.

Figure 7. Dependence of H^+ ion angular distribution on annealing temperature as examined by ESDIAD. (a) clean, prepared surface, as in Figs. 3(f) and 5(a); (b) after exposure to 10 L H_2; (c) after annealing to 601 K; (d) after annealing to 710 K; and (e) after annealing to 1041 K. All ESDIAD pattern were taken at 120 K with a $1x10^{-8}$ A, 300 eV electron beam. Elapsed time of data aquisition is 120 s.

Figure 8. The peak width of the ESDIAD pattern as a function of annealing (see Fig. 7). Note the peak width decrease after thermal removal of the β_3- and β_2-H_2 surface species (~700 K). This decrease is indicative of a surface species distribution involving a larger fraction of the monohydride (SiH) phase. Also note the sharply increased H^+ ESDIAD pattern width following annealing to 1041 K, where a highly-disordered Si surface is postulated to form, giving highly tilted Si-H bond directions.

Ultrahigh Vacuum Apparatus for Silicon Surface Chemistry

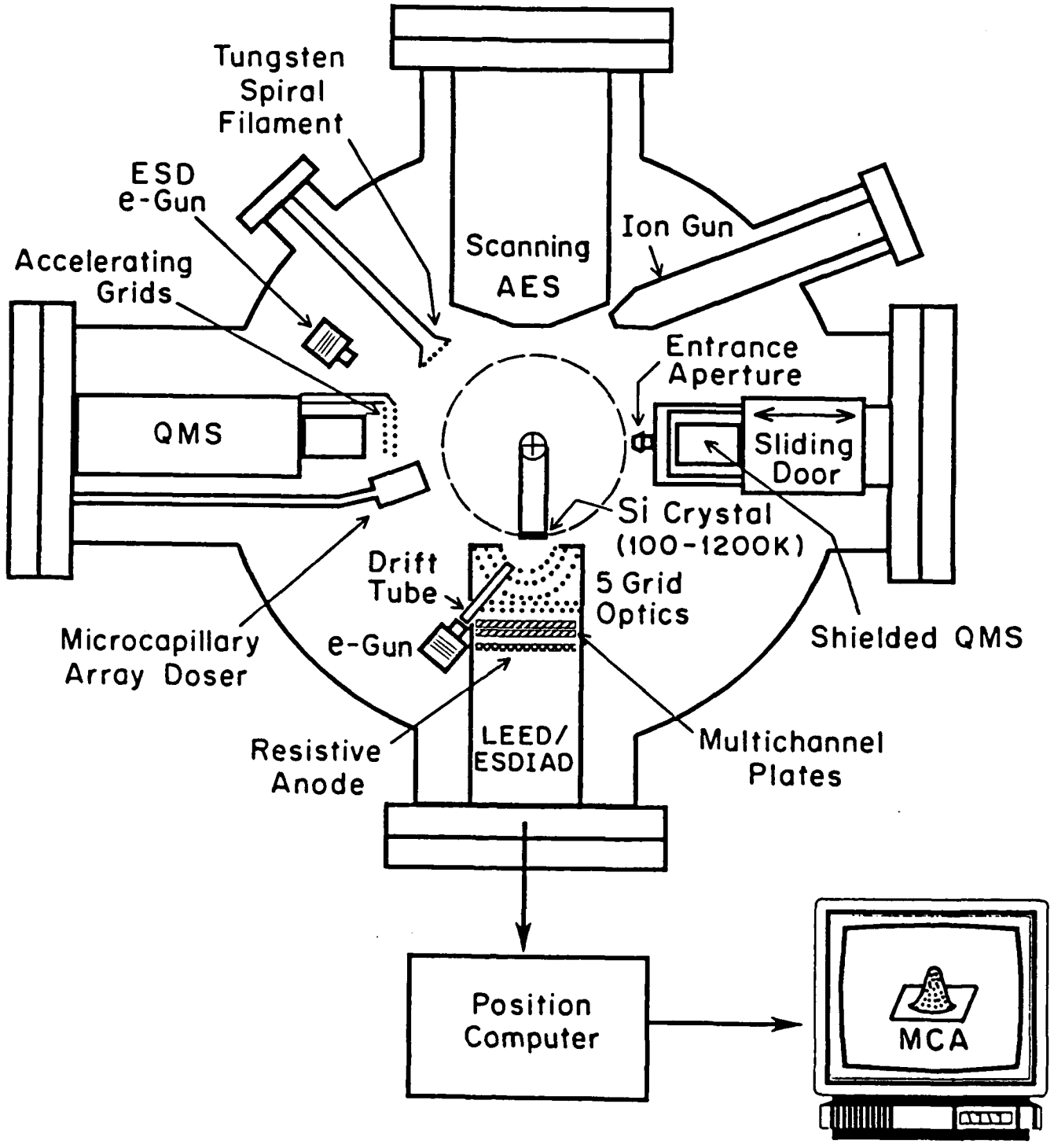

Wallace, et al
Figure 1

Cross-sectional View of Digital LEED/ESDIAD Apparatus

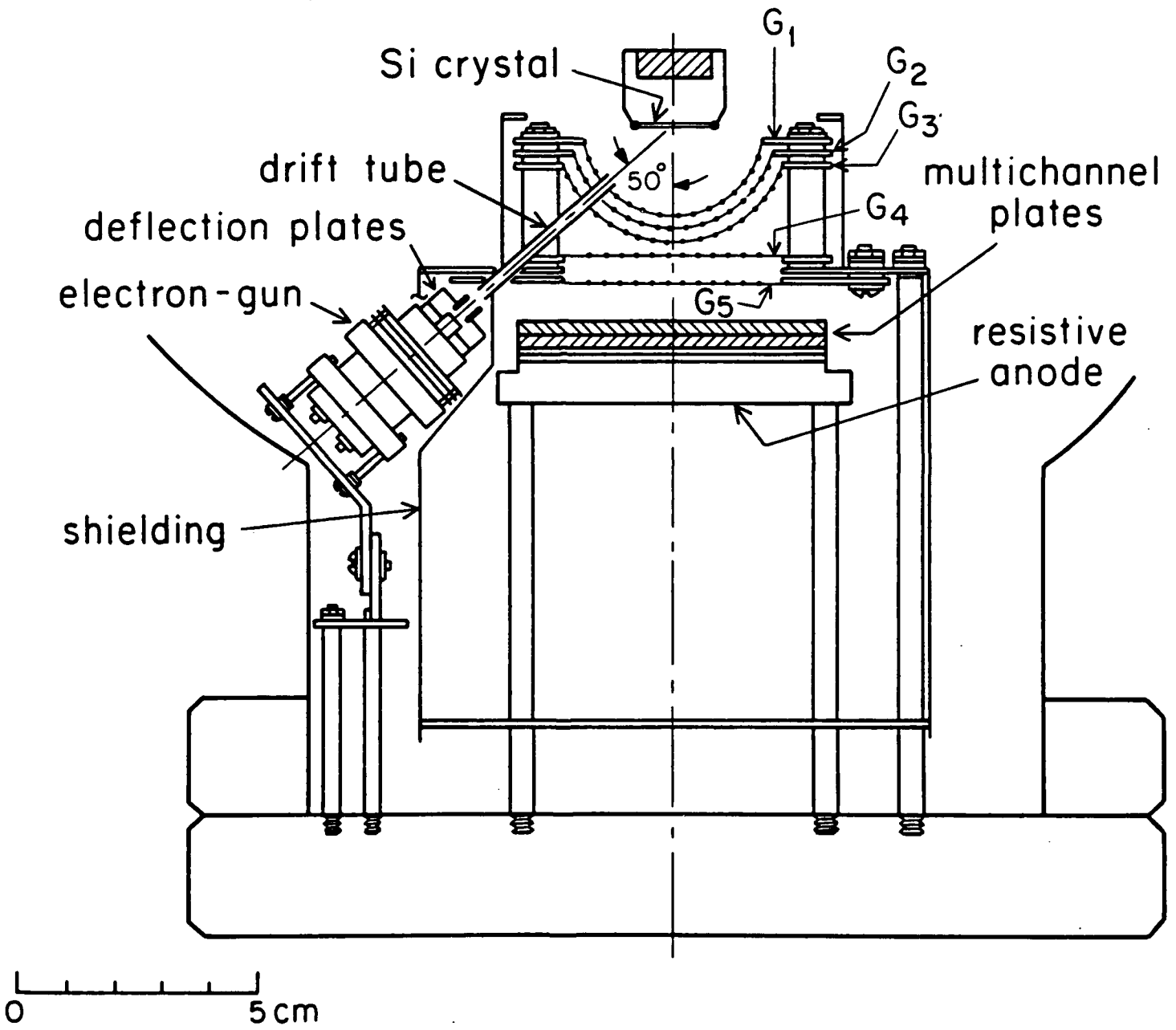

Wallace, et al
Figure 2

H^+ ESDIAD as a Function of Compression Voltage—Clean Si(111)—(7x7)

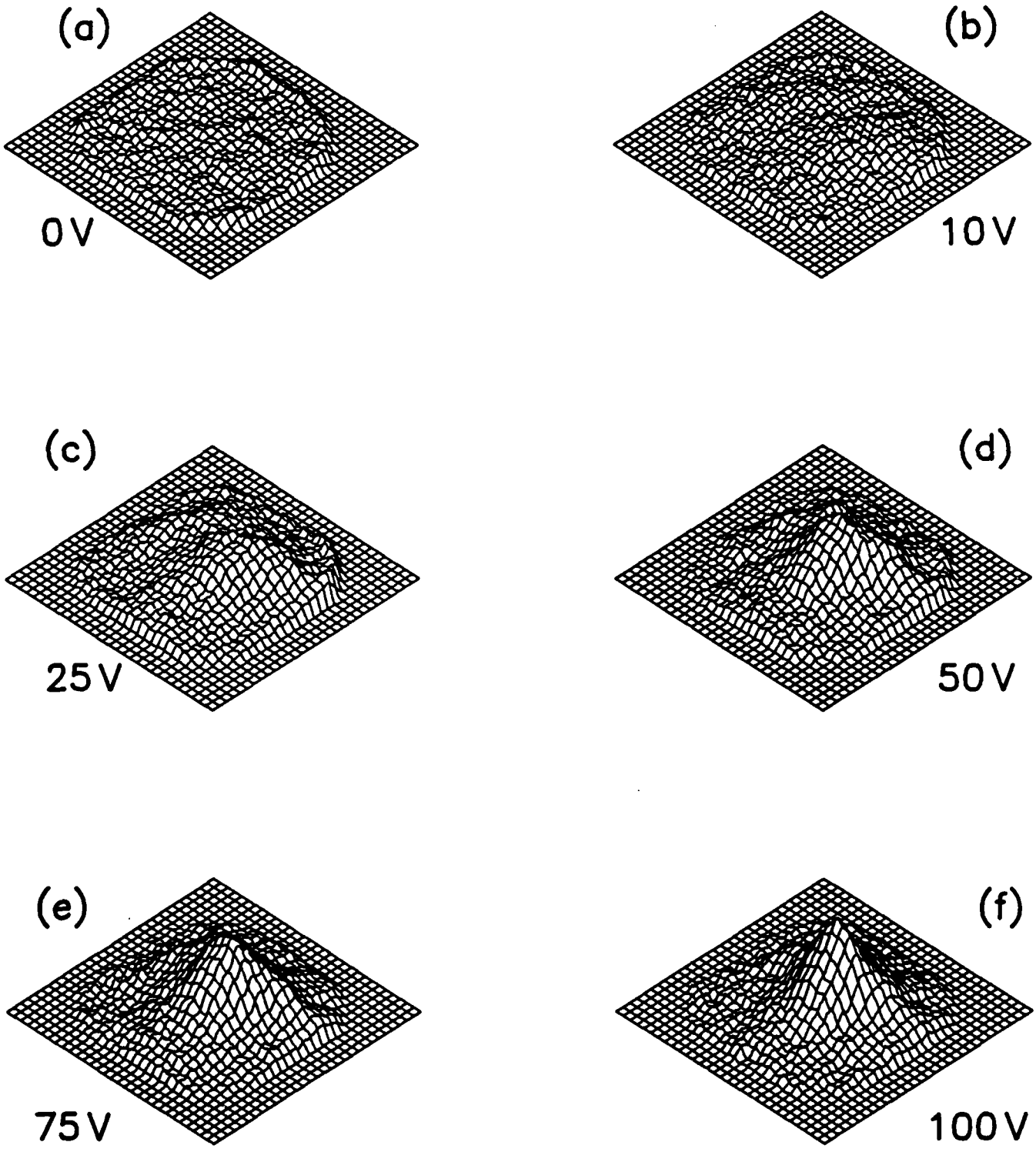

Wallace, et a.
Figure 3

Wallace, et al
Figure 4

H_2 Thermal Desorption Yield from "Clean" Si(111) after Multiple Temperature Programmed Desorption Cycles

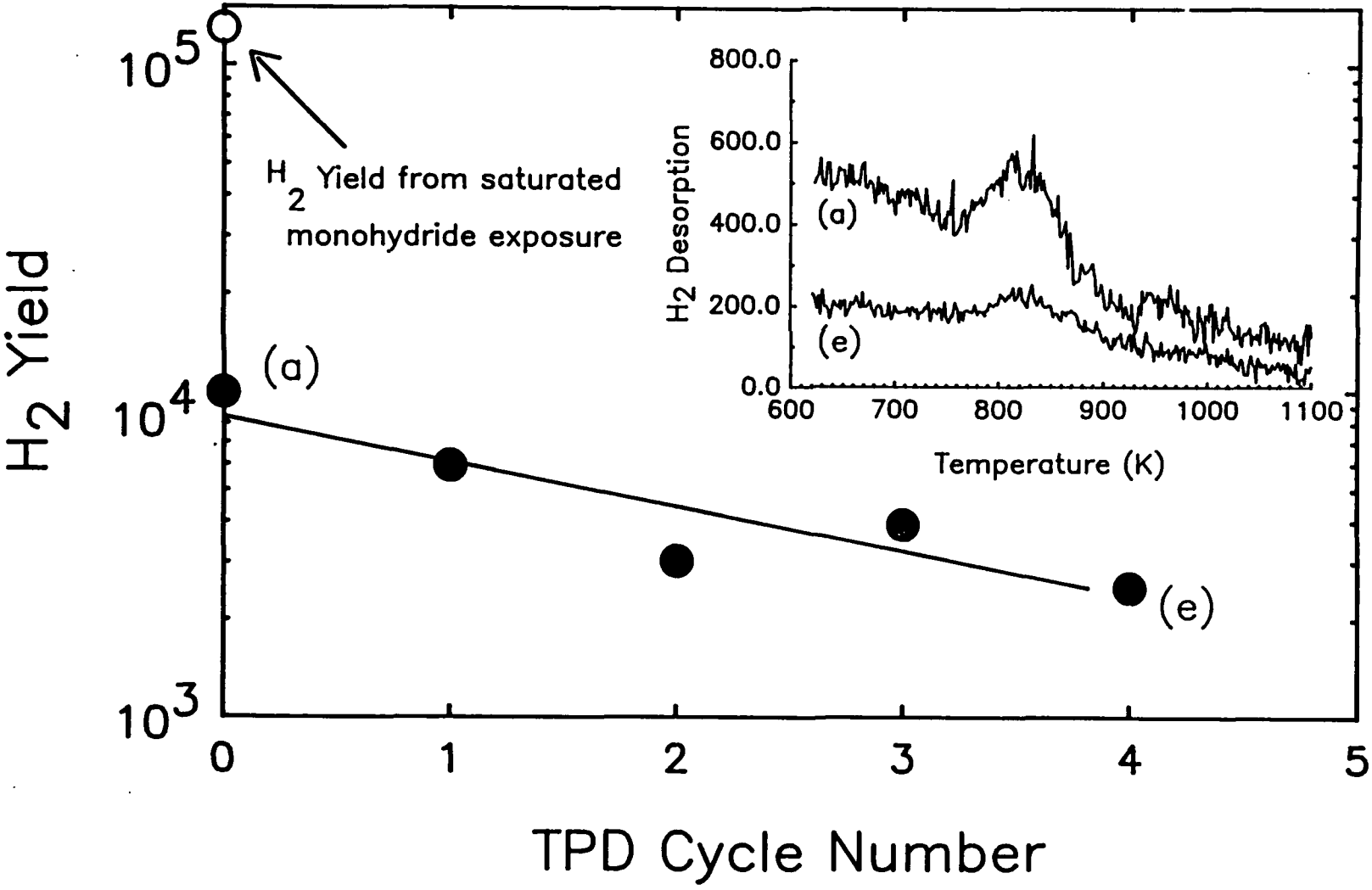

H^+ ESDIAD as a function of exposure to Atomic H–Si(111)–(7x7)

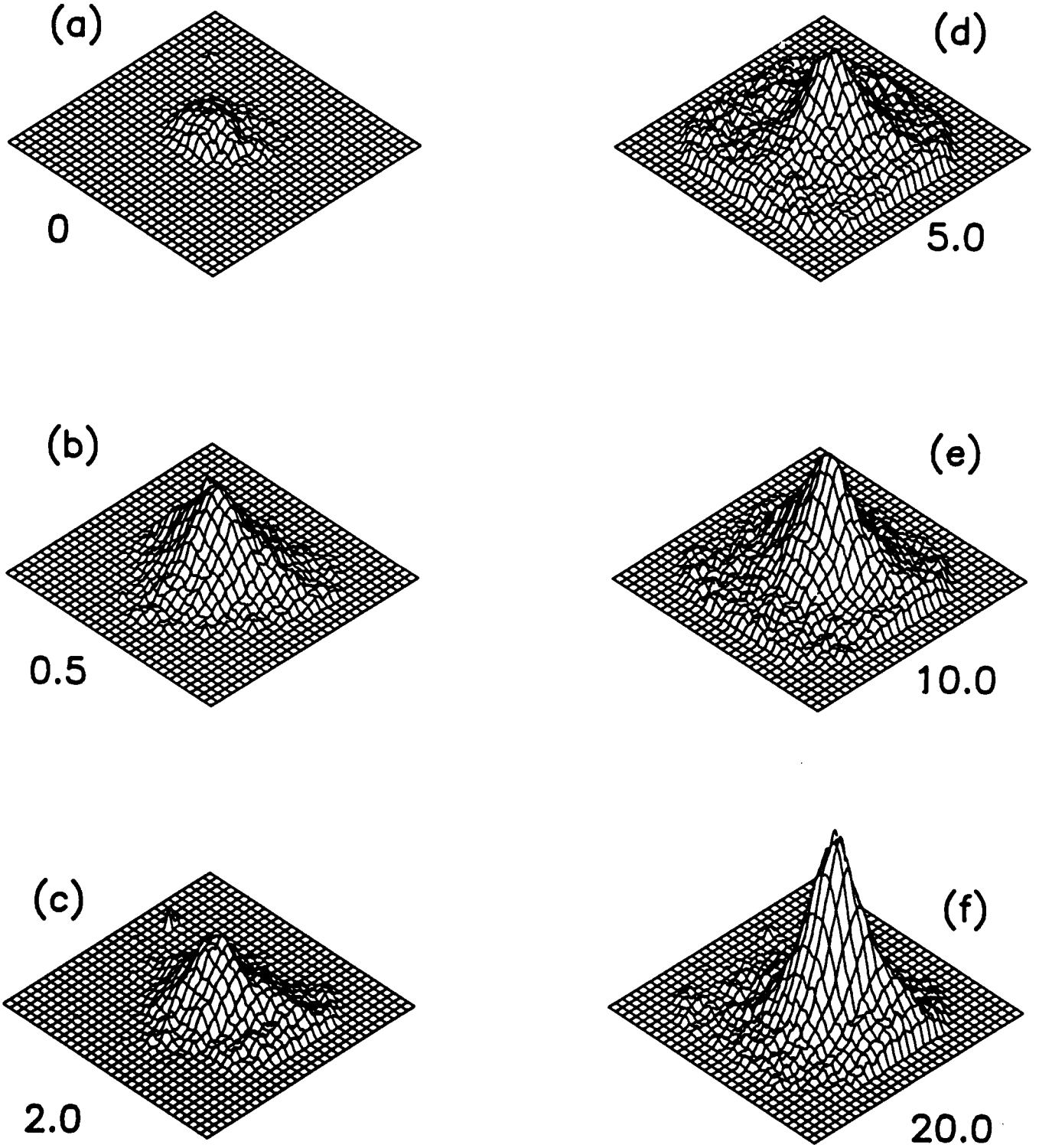

Wallace, et al
Figure 5

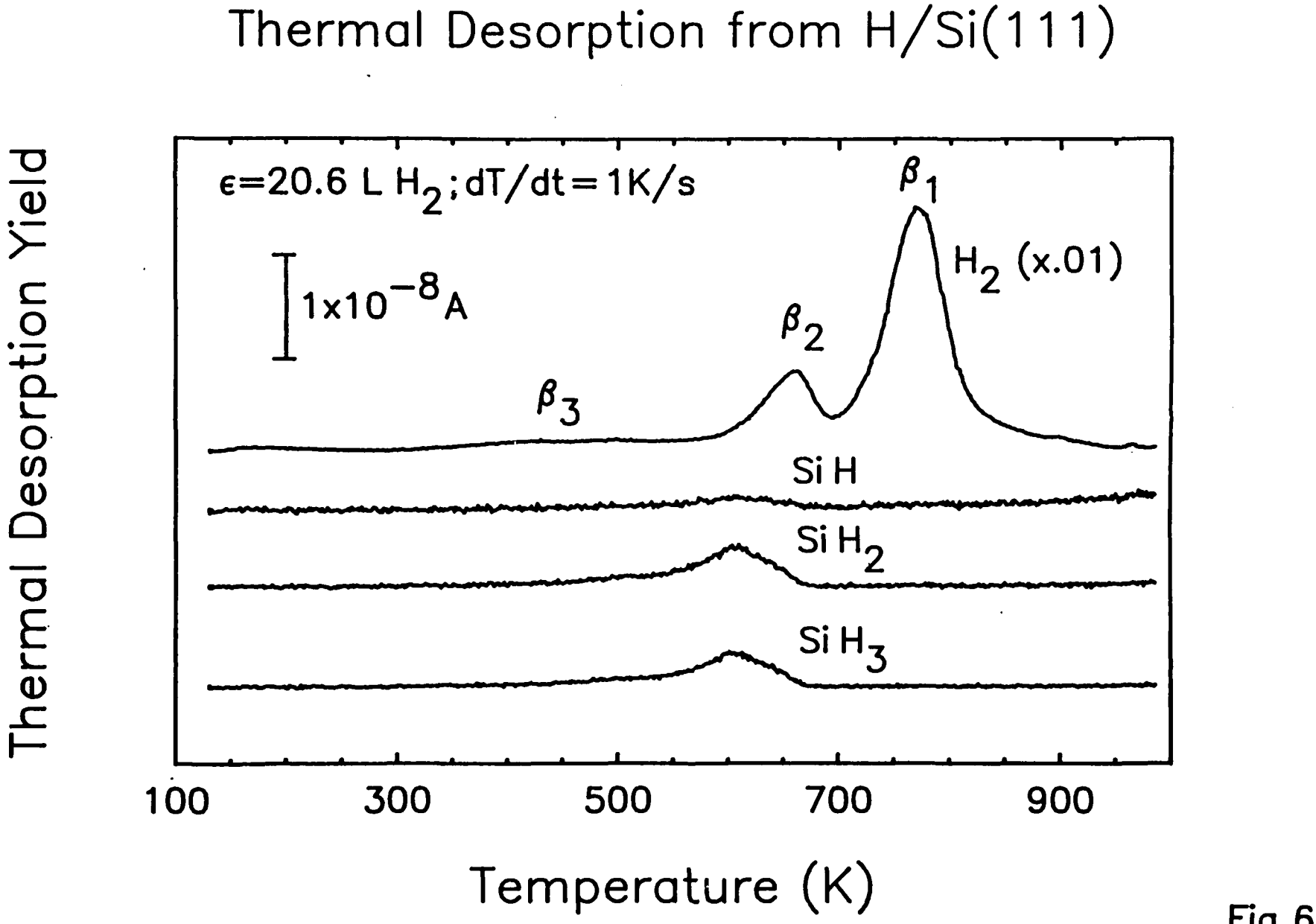
Thermal Desorption from H/Si(111)
Thermal Desorption Yield
ϵ=20.6 L H2; dT/dt=1K/s
1x10−8A
β1
H2 (x.01)
β2
β3
Si H
Si H2
Si H3
100
300
500
700
900
Temperature (K)

Fig 6

H^+ ESDIAD as a function of annealing—
H/Si(111)–(7x7)

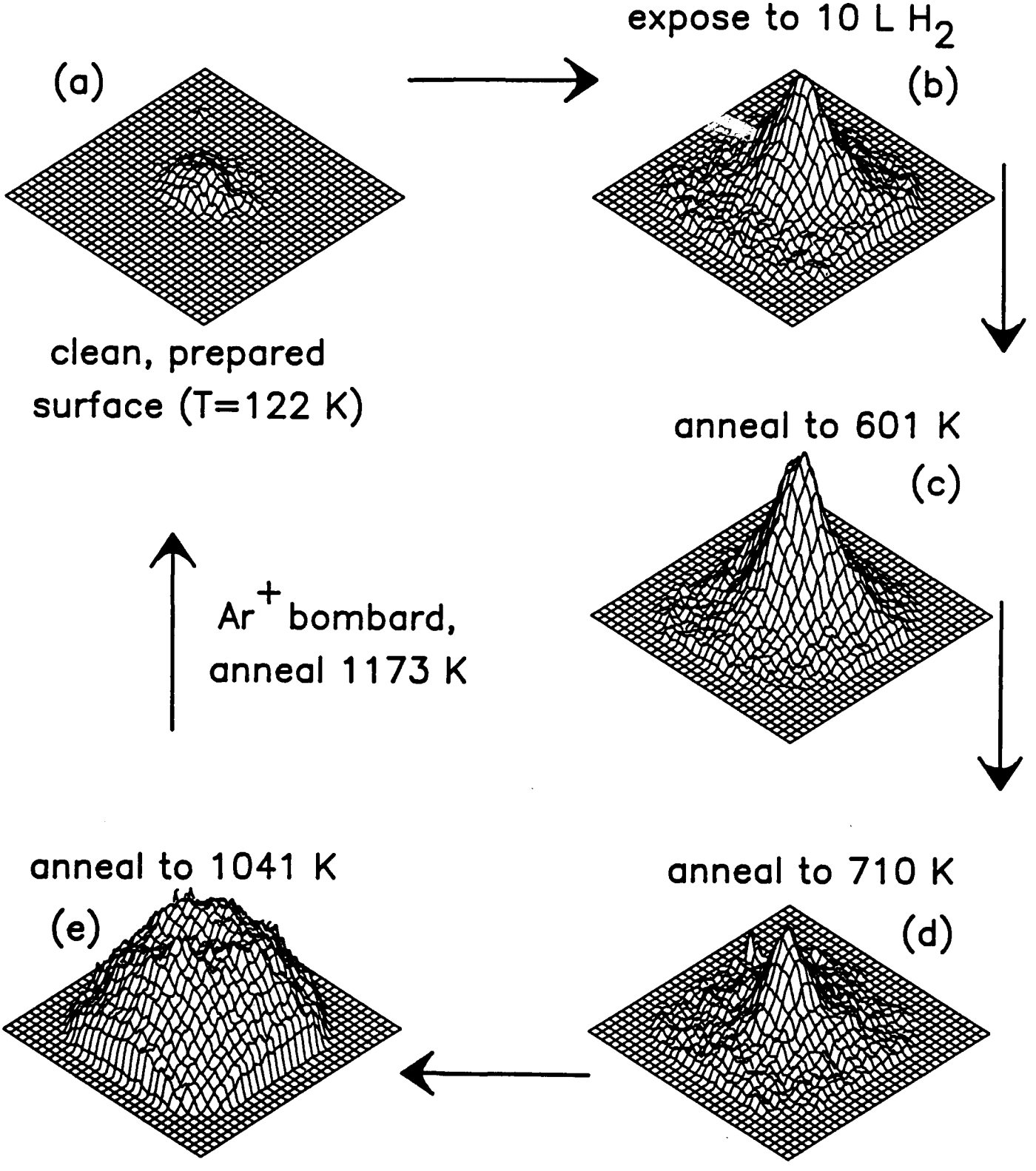

Wallace, et al
Figure 7

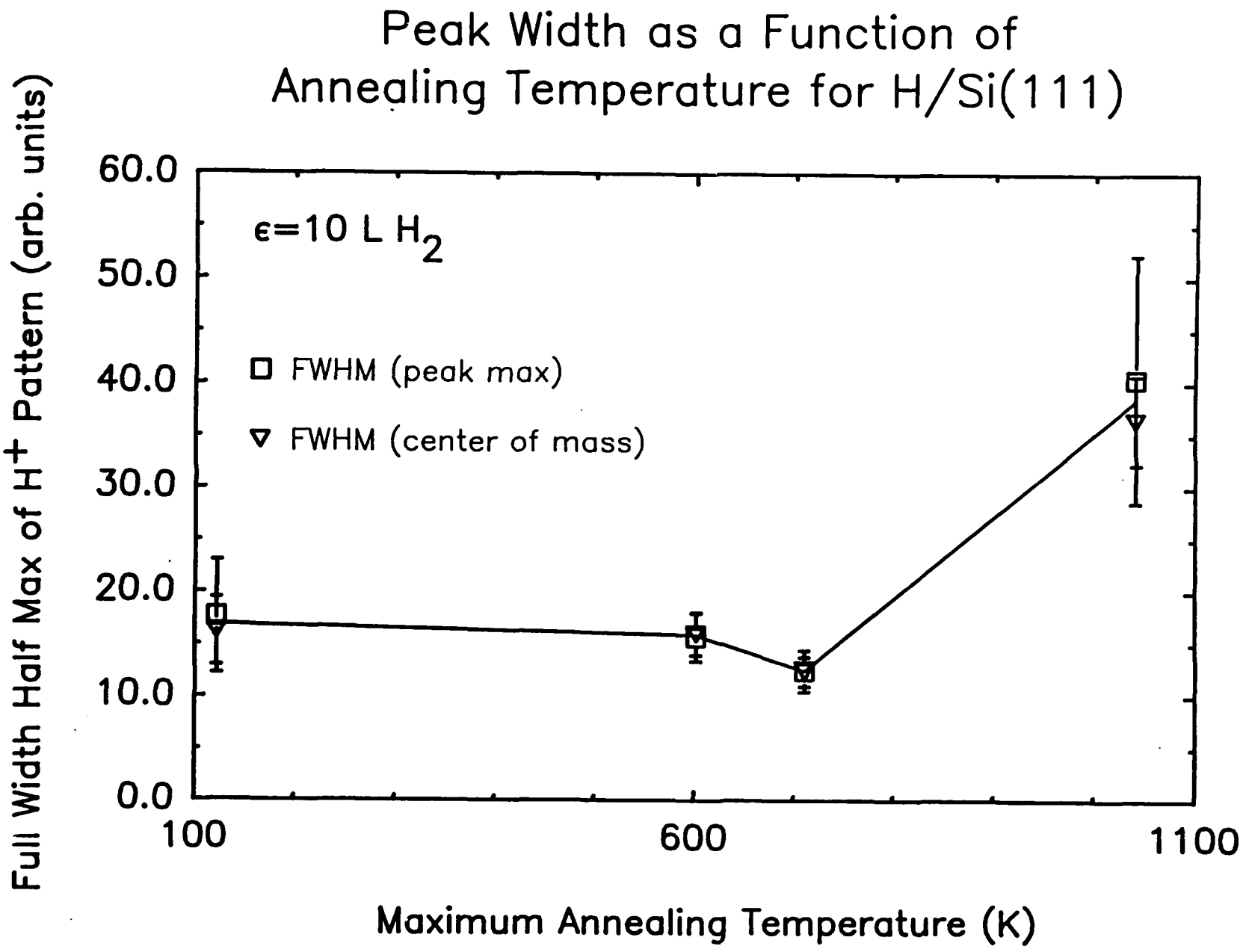

Wallace, et al
Figure 8

TECHNICAL REPORT DISTRIBUTION LIST, GEN

	No. Copies
Office of Naval Research Attn: Code 1113 800 N. Quincy Street Arlington, VA 22211-5000	2
Dr. Bernard Douda Naval Weapons Support Ctr. Code 50-C Crane, IN 57522-5050	1
Naval Civil Engr. Lab. Attn: Dr. R.W. Drisko Code L-52 Port Hueneme, CA 92401	1
Defense Technical Information Center Bldg. 5, Cameron Station Alexandria, VA 22314	12
DTNSRDC Attn: Dr. H. Singerman Applied Chemistry Division Annapolis, MD 21401	1
Dr. William Torres, Supt. Chemistry Div., Code 6100 Naval Research Laboratory Washington, DC 20375-5000	1
Dr. Mark Ross ONR 800 N. Quincy Street Arlington, VA 22217-5000	3
Dr. David Young Code 334 NORDA NSTL, Miss 39429	1
Naval Weapons Ctr. Attn: Dr. Ron Atkins Chemistry Division China Lake, CA 93555	1
Scientific Advisor (WF06B) Marine Corp-Ground Task Force Warfighting Center Marine Corps Combat Development Command Quantico, VA 22134-5001	1
U.S. Army Research Office Attn: CRD-AA-IP PO Box 12211 Res. Triangle Park, NC 27709	1
Mr. John Boyle Materials Branch Naval Ship Engr. Ctr. Philadelphia, PA 19112	1
Naval Oceans Systems Ctr. Attn: Dr. S. Yamamoto Marine Sciences Div. San Diego, CA 91232	1